

## Sol-gel coatings for optoelectronic devices

Cesar O. Avellaneda, Marcelo A. Macêdo, Ariovaldo O. Florentino, Michel A. Aegerter

University of São Paulo, Instituto de Física e Química de São Carlos, Cx. Postal 369, São Carlos (SP) - 13560-970 - Brasil

## ABSTRACT

$\text{Nb}_2\text{O}_5$  prepared by a sol-gel process in form of coatings and aerogels are new materials which present interesting properties: a) the coatings present electrochromic properties and exhibit a blue coloration under  $\text{Li}^+$  insertion with 100% reversible variation of the optical transmission in the visible and near infrared range between 80% and 20% and have a high chemical stability (tested up to 2000 cycles) b) they are semiconductor and present a photoelectric effect when illuminating in the UV region ( $\lambda < 360 \text{ nm}$ ). These films are therefore very promising to be used in electrochromic devices, as electrodes for photoelectrochemical purpose and the development of nanocrystalline solar cell. c) when prepared in aerogel form, the high BET surface area of the powders is a promising asset to use these new materials for catalytic purposes.

## 1. INTRODUCTION

The sol-gel process offers today many advantages over traditional techniques for the preparation of advanced and functional coatings having optical, electronic, chemical and mechanical functions [1]. Many sol-gel coatings are presently in practical use, especially for optical purposes.

In this paper, we briefly review the preparation and properties of some sol-gel coating materials which have been proposed in the last few years for the fabrication of electrochromic devices (a recent review on the applications of the sol-gel techniques to make solid state electrochromic devices has been reported by Agrawal et al [2]). We then report on the preparation and physical characteristics of functional  $\text{Nb}_2\text{O}_5$  films and discuss briefly some properties of aerogels and photoelectrical behavior of  $\text{Nb}_2\text{O}_5$  coating. Up to now these materials have been mainly prepared via conventional technique; however the sol-gel process, thanks to the variety of parameters which can be used and controlled during the sol preparation and gel fabrication, allows to obtain  $\text{Nb}_2\text{O}_5$  materials with interesting properties for electrochemical and chemical applications. The original results which are presented are not exhaustive and should stimulate more thorough studies to better understand amorphous and crystalline porous structures, a task for which the sol-gel technique appears today as most promising and unique.

## 2. SOL-GEL ELECTROCHROMIC COATINGS

A typical electrochromic device consists of five layers sandwiched between two glass substrates. There are two transparent electrical conductors required for setting up a distributed electric field, an electrochromic layer, an ionic conductor (electrolyte) and an ion ( $\text{H}^+$  or  $\text{Li}^+$ ) storage layer (counter electrode). When a small current is passed through the cell, the ions stored in the counter electrode diffuse toward the electrochromic layer and change its transmittance in the visible range. The original state is obtained by reversing the applied voltage.

Among the compositions which present an electrochromic behavior the oxides of transition metals such as  $\text{WO}_3$ ,  $\text{Nb}_2\text{O}_5$ ,  $\text{TiO}_2$ ,  $\text{V}_2\text{O}_5$ ,  $\text{TiO}_2\text{-CeO}_2$ ,  $\text{MnO}_2$ , and some mixed compounds appear to be the best materials; all have been already obtained via sol-gel process.

$\text{WO}_3$  coatings have been the most studied electrochromic materials [3, 4, 5, 6, 7, 8, 9, 10, 11]. At least four sol-gel routes have been developed for the preparation of sols to deposit  $\text{WO}_3$ : acidification of sodium tungstate [12, 13, 14], use of peroxopolytungstate acid [15, 16], reaction of tungsten chloride and oxo-chloride with alcohols [17, 18] and hydrolysis of alkoxides [19, 15]. According to Livage [6], the reaction of tungsten oxo-chloride ( $\text{WOCl}_4$ ) with isopropanol is the best method of preparation as it is a cheap technique and allows to obtain a sol stable for several months because of the formation of a molecular oligomeric precursor. Micrometer thick films of composition  $\text{WO}_3 \cdot n\text{H}_2\text{O}$  are easily obtained with control of the amount of water and the film morphology, which are essential for such application, by adequate heat treatments. The best electrochemical stability for  $\text{Li}^+$  insertion was encountered for  $n = 0.5$ , higher amount of water leads to a gradual decrease of the current indicating the occurrence of an irreversible process.

Using a sol prepared with a mixture of tungsten chloride ( $\text{WCl}_6$ ), titanium propoxide ( $\text{Ti}(\text{OPri})_3$ ) and ethanol, Götsche et al [20] have claimed a better electrochemical stability. However the addition of  $\text{TiO}_2$  (10-15 mol%) reduces the number of tungsten active sites and leads to a decrease of the reversible optical transmittance variation.

Using the methodology described by Livage's group [17], amorphous  $\text{WO}_3$  sol-gel films 200 nm thick heat treated at 120°C during 2 h. have been used by us to realized a complete sol-gel protonic smart window glass/ $\text{TiO}_2/\text{WO}_3/\text{TiO}_2/\text{CeO}_2/\text{TiO}_2/\text{glass}$  [21, 22]. The optical transmission and time response of the device during the first cycles were 60% <  $T$  < 20% at  $\lambda = 550 \text{ nm}$  and  $\sim 10 \text{ s}$  coloring and bleaching time respectively; the values were comparable to those obtained with windows built with non sol-gel coatings [23]. The main drawback was the lifetime of the device whose transmission variation  $\Delta T$  was gradually reduced with increasing number of cycles. The origin of this degradation is not known but is probably due to unwanted reaction at the  $\text{TiO}_2/\text{WO}_3$  interface [22]. Coating  $\text{WO}_3$  with a thin layer of  $\text{Ta}_2\text{O}_5$  [24] may offer a protection against such degradation. On the other hand, Livage et al [13, 25] have claimed a lifetime longer than 40000 cycles for a symmetric always colored cell  $\text{SnO}_2/\text{WO}_3/\text{TiO}_2/\text{SnO}_2$ , whose active layers have been realized with the same sol-gel methods.

Sol-gel electrochromic  $\text{V}_2\text{O}_5$  gels have been mainly synthesized by Livage's group using an alkoxide route [26, 27, 9]. The nature of the material was found to mainly depend of the hydrolysis ratio  $\text{H}_2\text{O}/\text{V}$ . The gels have mixed electronic and protonic conductivity and  $\text{Li}^+$  ions insertion is reversible. Mixed  $\text{V}_2\text{O}_5\text{-TiO}_2$  thin coatings have been prepared by Katsumi et al [28] with sols prepared from a mixture of V and Ti alkoxides in isopropanol and stabilized with the addition of acetylacetone and excess acetic acid. The electrochromic properties strongly depend on the atomic ratio  $x = \text{Ti}/(\text{V}+\text{Ti})$  and the calcination temperature. At 400°C for instance a two step coloration can be observed blue  $\rightarrow$  green  $\rightarrow$  yellow for  $x < 0.1$  and reddish-brown for  $0.6 < x < 0.67$ . At 500°C the coatings behave similarly to pure  $\text{V}_2\text{O}_5$ .

Amorphous  $\text{TiO}_2$  gel coatings prepared from hydrolysis and condensation of  $\text{Ti}(\text{OBu})_4$  [26, 29] exhibit reversible color-bleaching cycles and their color can be adjusted as grey or blue depending of the chemical additives used for the preparation of the sols. Ozer et al [30] using sols prepared with  $\text{Ti}(\text{isoPrO})_3$ ,  $\text{Ti}(\text{isoBu})_4$ , and acetic acid as catalysts also present electrochromism under certain preparation conditions.

Although they do not exhibit electrochromic properties, sol-gel coatings of  $\text{CeO}_2$  [31] and mixed  $\text{TiO}_2\text{-CeO}_2$  [31, 21, 22] have high electrochemical reversibility for  $\text{Li}^+$  ions and have been proposed for ions storage electrodes. Pure  $\text{CeO}_2$  coatings shows larger storage capability [31].

Fig 245

## 2.1 Nb<sub>2</sub>O<sub>5</sub> sol preparation and coating characterization

Sol-gel Nb<sub>2</sub>O<sub>5</sub> films are new very promising candidate for electrochromic coatings. Very few studies have been reported on the electrochromic properties of Nb<sub>2</sub>O<sub>5</sub>. Reichman and Bard [32] showed the occurrence of such effects in a 15 μm thick coating produced on the surface of a niobium metallic disk by heating at ~500 °C for about 10 min. A coloring effect, chemically stable and with a fast kinetics (1-2s) was seen in reflexion under either H<sup>+</sup> or Li<sup>+</sup> insertion. Gomes et al. [33] have studied in details the protonic electrochromic properties of 20 μm thick opaque coating prepared in the same way and later Alves [34] has confirmed the possibility to insert Li ions in a 1 mm thick Nb<sub>2</sub>O<sub>5</sub> ceramic prepared from commercial CBMM powder sintered at 800°C.

The first attempt to fabricate sol-gel Nb<sub>2</sub>O<sub>5</sub> for electrochemical purpose has been reported by Lee and Crayston [35] who have spin coated ITO coated glass electrode with a mixture of NbCl<sub>5</sub> dissolved in EtOH. Hydrolysis and gelation were completed in 1 mol/dm<sup>3</sup> H<sub>2</sub>SO<sub>4</sub> solution. After drying at room temperature the result was a 5-10 μm thick film with substantial cracking (10 μm islands) and peeling due to important shrinkage. Cyclic voltammograms in LiClO<sub>4</sub>-MeCN electrolyte showed a blue coloration with a fast coloration (~ 6s) and bleaching (~ 3s) kinetics and a 6 cm<sup>2</sup>/C coloring efficiency. However the durability of the electrochromic response was only a few cycles. The quality of the film has been slightly improved by adding a trialkoxysilane (Glymo) to the precursor sol in order to obtain a Nb-Si Ormocer.

In our laboratory, Nb<sub>2</sub>O<sub>5</sub> sols have been prepared using an alkoxide route (figure 1a). Pentabutoxide of niobium (Nb(OBu)<sub>5</sub>) was first synthesized following the process described by Bradley et al. [36] by dissolving niobium chloride (NbCl<sub>5</sub>) from CBMM-Brazil in butanol and then mixed with sodium butoxide (Na(OBu)<sub>3</sub>) under reflux. During the process a strong exothermic reaction occurs leading to the formation of Nb(OBu)<sub>5</sub> and NaCl. The last compound was then separated by centrifugation to obtain a yellow and transparent precursor sol. The final sol was prepared by mixing this precursor with glacial acetic acid (CH<sub>3</sub>COOH) with molar ratio 1:2 resulting in a sol stable at room temperature for several month. [37]. The coatings have been deposited by dip coating technique on Donnelly or Asahi Glass ITO coated glass at a withdrawal speed of 12 cm/min, dried at room temperature during 5 min and then densified at 400°C during 15 min. They have typically a thickness of ≈ 80 nm. The process has been repeated three times to obtain a 250 nm thick film; the final coating has been finally heat treated in O<sub>2</sub> atmosphere between 400 and 600°C. [21, 37]. Figure 1b shows a block diagram of this procedure.

Figure 2 shows a typical SEM micrograph and EDX scan of Nb (taken at the location of the line shown on the micrograph) of a three layers Nb<sub>2</sub>O<sub>5</sub> film (250 nm thick) obtained according to the above procedures with a heat treatment at 560°C in O<sub>2</sub> atmosphere during 2 h. The picture shows very good homogeneity of the Nb atoms and excellent microstructure of the surface with no visible cracks and defects.

X-ray diffractograms of xerogels obtained with the same sol have been obtained with a Rigaku model RU200B instrument with a Kα Cu radiation. Figure 3 shows that the gels heat treated up to 500 °C are amorphous. At 560 °C the material is crystalline but the lines are poorly defined. Their position and intensity are compatible with the so-called TT phase as can be seen by comparison with the top part of the figure [38,39]. The width of the principal lines somewhat sharpens at 600 °C but the overall shape of the spectrum does not change. No trace of other phases (T<sub>1</sub>M<sub>1</sub>H) has been observed. According to Ko [38], the TT phase is not strictly a niobium pentoxide as some oxygen atoms are replaced by monovalent species such as X = OH<sup>-</sup>, Cl<sup>-</sup>, vacancies etc. and Nb atoms occupy separated but closely-spaced equivalent sites or intermediate positions between them; the compound should be better denoted Nb<sub>16</sub>O<sub>38</sub>X<sub>4</sub> or Nb<sub>4</sub>(OX)<sub>5,m</sub>. DSC and DTA measurements (TA 9010 Instrument) made at 2 °C/min in a O<sub>2</sub> flux confirm the presence of a small crystallization peak at ~ 580°C (formation of the TT-phase) followed by an intense peak with maximum at

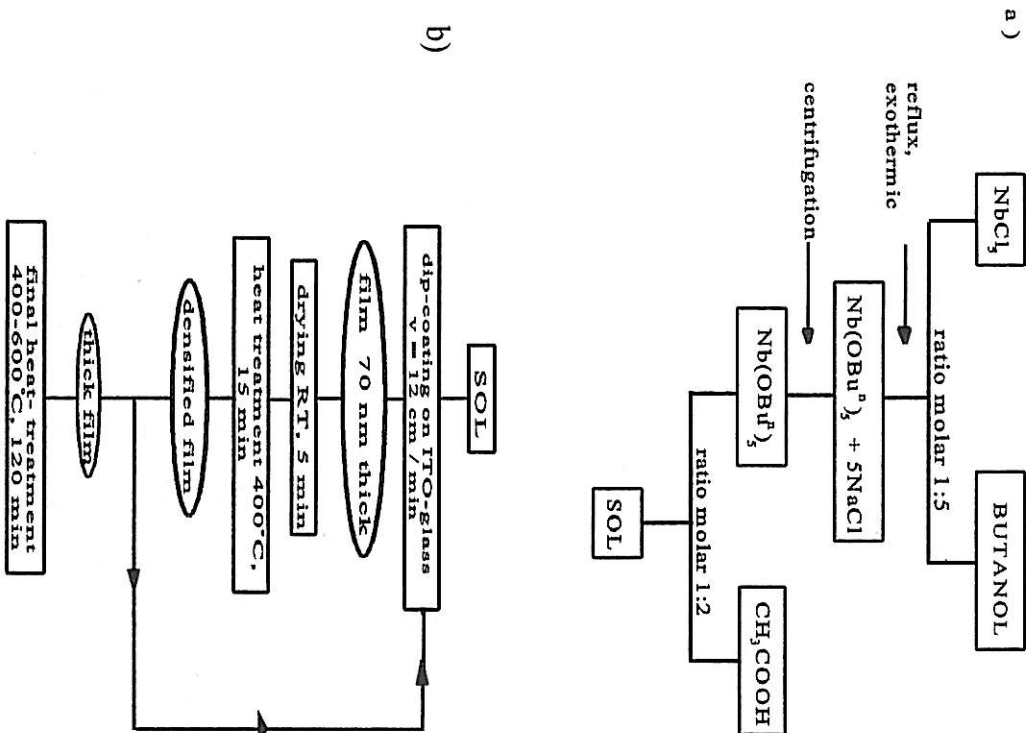


Fig. 1 Block diagram of a) Nb<sub>2</sub>O<sub>5</sub> sol preparation and b) Nb<sub>2</sub>O<sub>5</sub> film preparation.

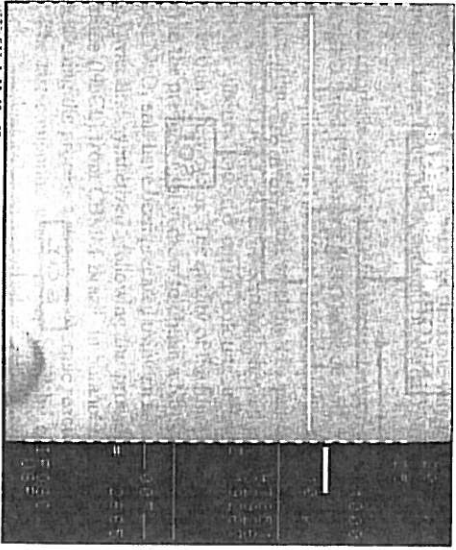
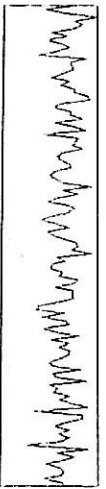


Fig. 2 Scanning electron micrograph of a 3 layers  $Nb_2O_5$  250 nm thick deposited on glass/ITO (Donnelly) substrate heat treated at 560°C during 2h in  $O_2$  atmosphere and EDX line scan of Nb.

630°C (probably due to the transformation  $TT \rightarrow T'$ ).

Figure 4 presents typical voltammograms measured at speed varying from 2 to 200 mV/s between +2.0 and -1.8 V/vs Ag/AgCl reference) for a 3 layers  $Nb_2O_5$  coating deposited on ITO coated glass (Asahi Glass) and sintered 2 h at 560°C in oxygen. The measurements have been performed with a Solartron 1226 electrochemical interface and a cell consisting of three electrodes: a Pt foil ( $1\text{ cm}^2$ ) as counter electrode, an Ag/AgCl as a quasi-reference electrode and the " $Nb_2O_5$ " film as working electrode (working area  $0.3\text{ cm}^2$ ). The electrolyte was  $LiClO_4$  dissolved in propylene carbonate with concentration 0.1M and has been previously purged with dry  $N_2$  gas. All the electrochemical measurements have been done in a dry box containing  $N_2$  atmosphere with less than 100 ppm  $H_2O$ . We must first mention that the voltammograms could not be registered at potential value lower than -2.0 V. Below this value the cathodic current increases very rapidly, the coating turns black and is permanently damaged. Electrochemical measurements made with uncoated but heat treated ITO substrates shows that this effect is due to the reduction of this material. Within the safe range of -1.8 to 2.0 V, two different regimes can be observed.

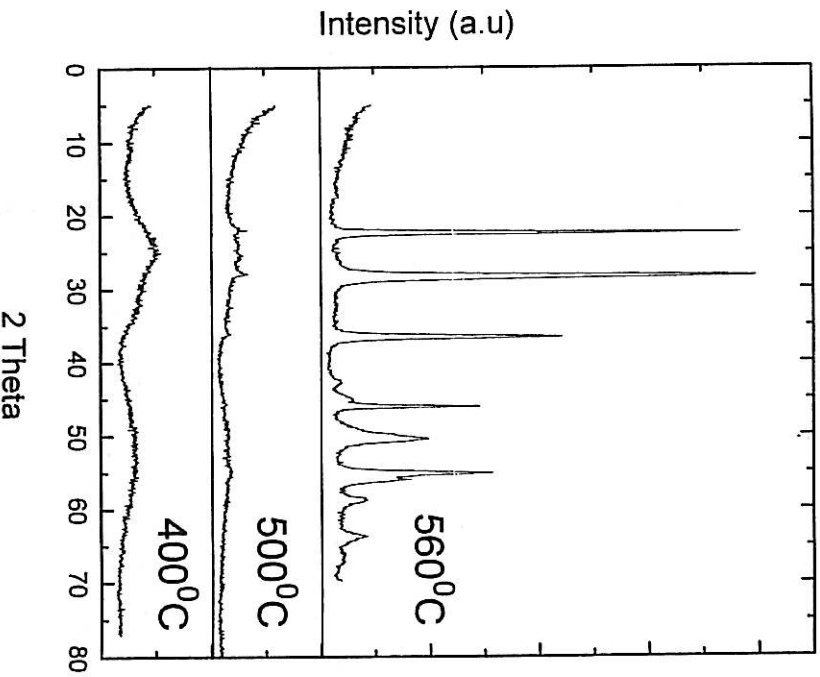
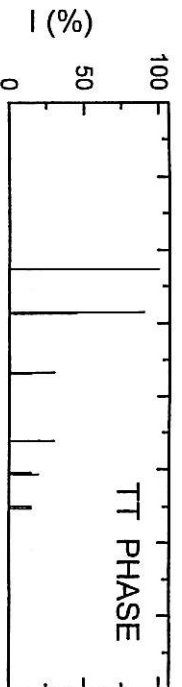


Fig. 3 Lower part: X-ray diffraction of  $Nb_2O_5$  xerogels heat treated at 400, 500, 560°C during 2h in  $O_2$  atmosphere. The top part shows the position of the principal peaks of the TT phase

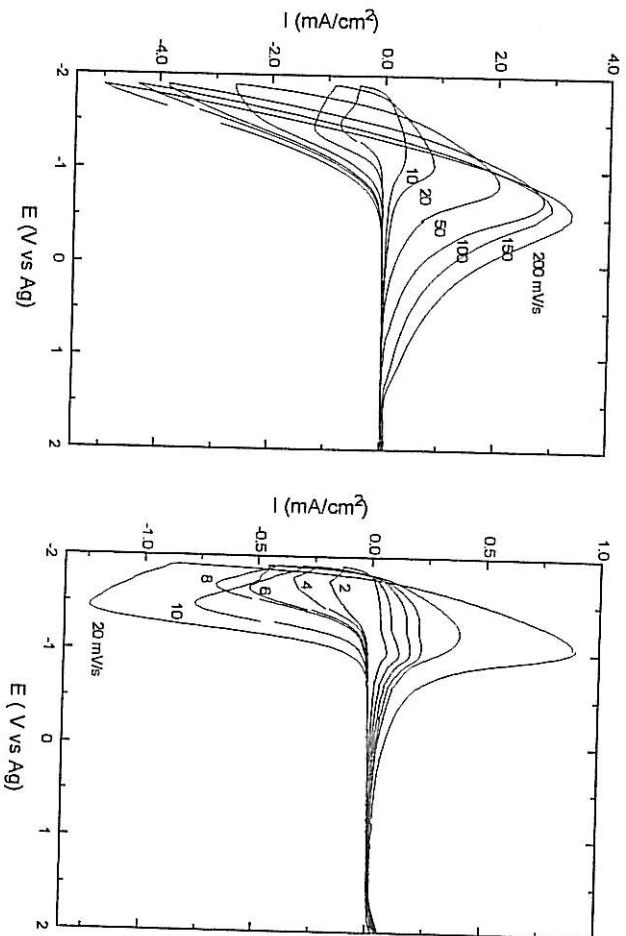


Fig. 4 Voltammograms of a 250 nm thick  $\text{Nb}_2\text{O}_5$  coating deposited on a glass/ITO (Asahi Glass) substrate and heat treated at 560 °C during 2h in  $\text{O}_2$  atmosphere. Electrolyte  $\text{N}_2$  purged 0.1M  $\text{LiClO}_4/\text{PC}$ ; reference  $\text{Ag}/\text{AgCl}$ , potential scan +2 V to -1.8 V a) scan rates 2,4,6,8,10,20 mV/s and b) scan rates 10,20,50,100,150 and 200 mV/s.

At low speed ( $v < 10$  mV/s) the curves are rather complex and appear as a superposition of at least two insertion phenomena, one into the niobate coating and the other into the ITO coating to which belong the cathodic and anodic waves observed at -1.7 and -1V respectively (figure 4a). BET measurements (not shown here) indicate that xerogels have still at 560 °C a relatively high porosity and as the charge inserted,  $Q_{\text{c}}$ , is high and constant ( $Q_{\text{c}} = 20$  mC/cm $^2$ ), as shown in figure 5, it seems that, at these low scan rates, the  $\text{Li}^+$  ions have time to reach the electronic coating. On the other hand, as shown in the same figure, the cycles are not reversible: the total charge extracted,  $Q_{\text{a}}$ , is smaller than the total charge inserted and consequently the ratio  $Q_{\text{a}}/Q_{\text{c}}$  is smaller than 1. The color of the coating after Li insertion is blue-black and after bleaching the system remains slightly colored.

For scan rate higher than 10 mV/s the voltammograms are totally different (figure 4b). At lower speed the Li insertion peak is clearly visible, but shifts rapidly to lower and out of range potentials when the speed is increased. The extraction peak can be observed in the whole scan range and also shifts but to higher potential values. Although the value of the charge inserted or extracted diminish with the speed, their ratio  $Q_{\text{a}}/Q_{\text{c}}$  remains now constant and approximately 1 (figure 5) indicating that the process is fully reversible in this speed range.

The variation of the maximum intensity of the cathodic and anodic currents with the scan rate is practically impossible to measure as at low speed it is necessary to make a careful deconvolution of the insertion processes and at high speed, the maximum of the insertion peak is not observed in the safe potential range used and the values of  $I_{\text{max}}$  of the extraction peak should be measured from the base line of the cathodic part at low negative potential, a task which is impossible to realize without a better knowledge of the chemical processes occurring at the electrode. Therefore it is not possible to argue if the process is limited by the Li diffusion or is due to a superficial phenomenon. Measurements are underway with coatings deposited on metallic substrate in order to avoid the ITO reduction occurring at  $\approx -2.0$  V and extend the potential range to lower values.

In this speed range and after Li insertion the color of the coating is deep blue. Figure 6 shows the optical transmission spectrum measured in situ with a Cary 17 spectrophotometer in the range 300 to 1100 nm at different applied potentials either during the insertion or the extraction process. A small hysteresis is observed but the good superposition of the curves in the bleached state at +2.0 V shows that the system is totally reversible.

Figure 7 shows the result of a chronoamperometry where the current was registered during the application of a square pulse of +2.0 to -1.8 V. The insertion process has a time response of about 10 s while the extraction process is faster, about 4 s.

For coatings deposited either on Asahi Glass or Domnelly ITO and heat treated in  $\text{O}_2$  atmosphere the charge is constant since the first cycles and the temporal behavior tested up to 2000 cycles shows an excellent chemical stability (figure 8). When the coatings are amorphous (i.e. for heat treatment at  $T \leq 500$  °C), the inserted (or extracted) charge first increases up to about 500 cycles and then decreases; this behavior suggests some structural evolution of the amorphous oxide network. The shape of the voltammograms measured at 50 mV/s are similar to that shown in figure 4b but the color of the layer is brown and the amount of charge inserted is smaller. When the coatings are heat treated in air instead of  $\text{O}_2$  at temperature between 400 and 560 °C, we found that the amount of charge slightly decreases with the number of cycles for both type of substrates. It is also possible to insert proton in these coatings. The cycles are also reversible but the lifetime of the coatings is short and does not exceed a few cycles. We believe that the bad performance is due to corrosion problems as it is with  $\text{WO}_3$  coating.

In conclusion we can state that "niobate" coating can now be prepared by the sol-gel process with excellent optical quality without cracks and good homogeneity. These coatings show reversible electrochromic properties when measured at scan rate higher than 10 mV/s and exhibit a deep blue coloration similar to that of  $\text{WO}_3$  coating. The variation of the optical transmission is high for a 250 nm thick layer and the kinetics of the

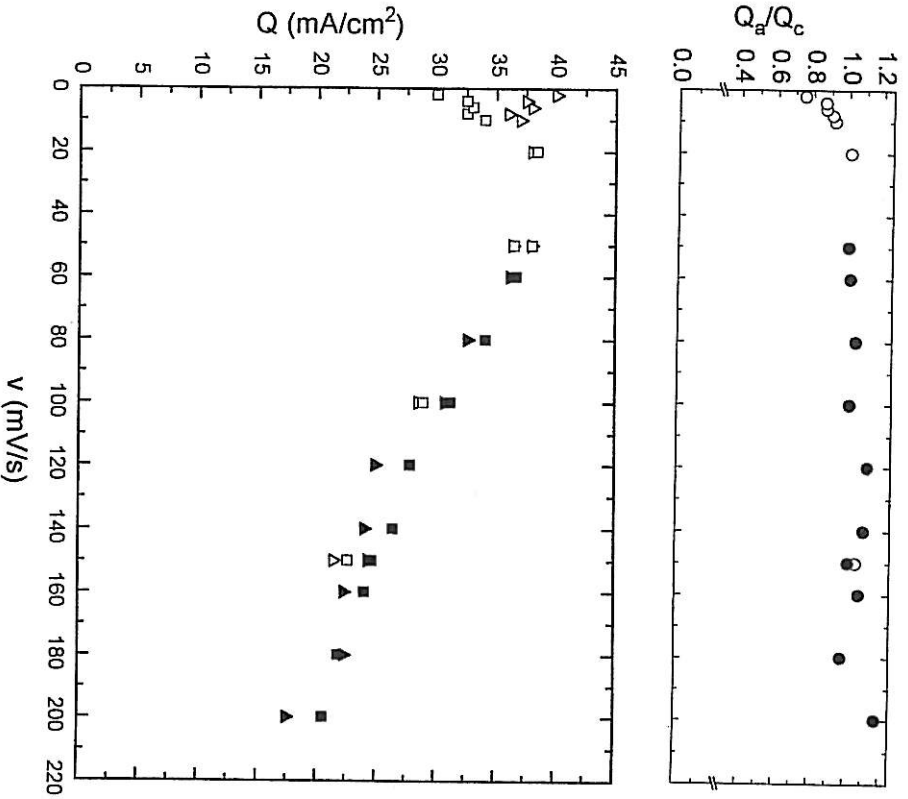


Fig. 5 Lower part : Inserted charge  $Q_c$  ( $\blacksquare, \blacktriangle$ ) and extracted charge ( $\blacktriangle, \triangle$ ) integrated from the voltammograms obtained with two films prepared in the same conditions versus scan rate. Upper part : ratio  $Q_a/Q_c$  versus scan rate.

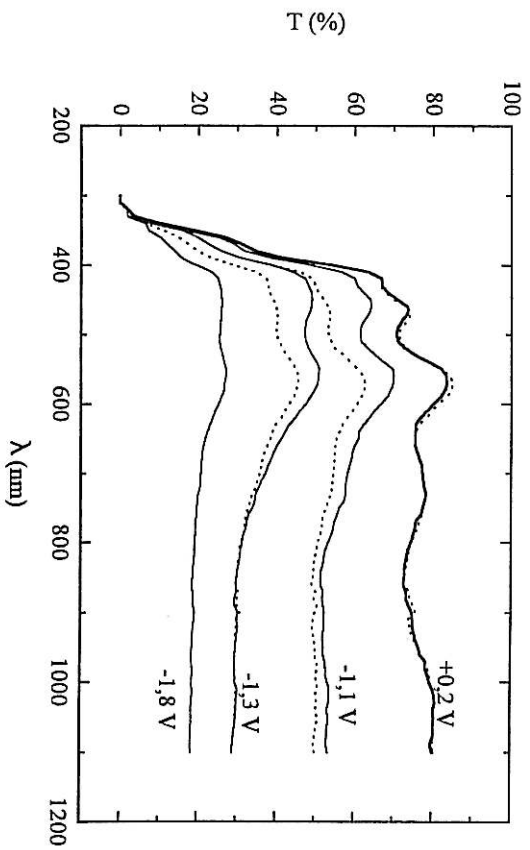


Fig.6 Optical transmission spectrum of  $Nb_2O_5$  coating heat treated at  $560\text{ }^\circ\text{C}$  during 2h in  $O_2$  atmosphere and measured after different step potentials during a complete cycle.

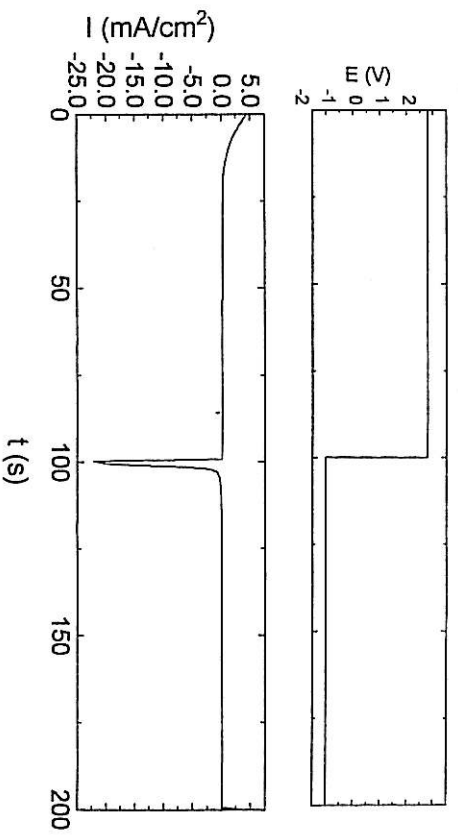


Fig. 7 Chronoamperometry of  $Nb_2O_5$  coating heat treated at  $560\text{ }^\circ\text{C}$  during 2h in  $O_2$  atmosphere (same electrochemical conditions as figure 4).



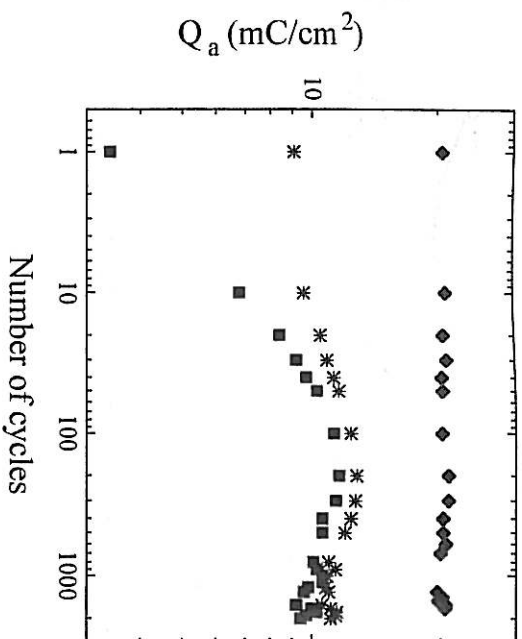


Fig. 8 Time dependence of the charge inserted (or extracted) as a function of the number of voltammetry cycles (+2V to -1.8 V) measured at a scan rate of 50 mV/s. The coatings have been heat treated for 2h in O<sub>2</sub> atmosphere at (◻) 500 °C (crystalline), (◼) 500 °C (amorphous) and (◊) 400 °C (amorphous).

insertion and extraction processes is quite adequate to use these coatings as electrochromic layer to built smart windows or mirrors, a research which is presently underway in our laboratory.

### 3. SOL-GEL Nb<sub>2</sub>O<sub>5</sub> AS CATALYST

Niobate materials in a wide variety of forms have been recently found active for many catalytic reactions [38]. When incorporated to V<sub>2</sub>O<sub>5</sub>, the most popular catalyst for decomposition of NO in the industrial stack gas to prevent air pollution, Nb<sub>2</sub>O<sub>5</sub> has been shown to have a *promoting* effect.

Remarkable *support* effect was reported on Rh catalyst for activity and selectivity toward higher cations in Co+H<sub>2</sub> reaction. Nb<sub>2</sub>O<sub>5</sub> deposited on Ni shows much higher conversion than Ni/Al<sub>2</sub>O<sub>3</sub> catalyst for CO hydrogenation and Pd and Co/Nb<sub>2</sub>O<sub>5</sub> catalysis are for instance more interesting than Al<sub>2</sub>O<sub>3</sub> for the synthesis of methylisobutyl ketone from acetone. However the most interesting properties of Nb<sub>2</sub>O<sub>5</sub> arise from its high acidic behavior when hydrated. When calcined at 100-300°C, Nb<sub>2</sub>O<sub>5</sub>·nH<sub>2</sub>O exhibits a high acid strength (H<sub>a</sub> = -5.6) corresponding to the acid strength of 70% H<sub>2</sub>SO<sub>4</sub>; this material is expected to show high and stable catalytic

activity for acid catalyzed reactions in which water molecules participate or are liberated such as the hydration of ethylene into ethylalcohol for instance.

For these applications, it is evident that the surface area of the materials should be as high as possible. The material, as produced in powder form by CBMM (Brazil) has a typical value S=75-100 m<sup>2</sup>/g. The preparation of highly porous materials using supercritical drying of gels, a technique which has mainly been applied to the preparation of silica aerogel[40], is one of the method which can be used to obtain materials with higher surface area.

The preparation of sol to obtain Nb<sub>2</sub>O<sub>5</sub> aerogel, has been slightly modified. The niobium alkoxide (Nb(OC<sub>2</sub>H<sub>5</sub>)<sub>5</sub>, prepared as above, was first hydrolyzed at room temperature with bidistilled water and HNO<sub>3</sub> under mechanical stirring using molar ratio H<sub>2</sub>O/Nb = 10 and HNO<sub>3</sub>/Nb = 0.8. The sol was let to gel during 7h. Nb<sub>2</sub>O<sub>5</sub> aerogels have been then obtained by supercritical drying using CO<sub>2</sub> as extracting agent at 60 atm and a critical temperature of 250°C. The CO<sub>2</sub> flux was adjusted to 6 l/h and the time of extraction was 1 h. Calcination of the aerogel has been performed in air.

The values of the BET surface area of aerogel heat treated at 300°C during 12 h are almost 2.5 times larger than the commercial (CBMM-AD638) product and remain practically constant up to 500°C while for the CBMM product the value has been already reduced to one half. More interesting is the fact that the ratio of the surface area (Saerogel) / S(CBMM) is about 2 at 300°C, increases to 4 at 500°C and remains 4 up to 700°C although both compounds suffer a drastic decrease of their S values. The supercritical drying process appears therefore to delay considerably the densification process and allows to maintain a more open structure.

Modifications have also been observed on the crystalline structure and the morphology of the materials. At 500°C the commercial product has a mixed crystalline structure of type T and TT [38] while the aerogel is still practically amorphous. At 700°C both structures are crystalline. The morphology of the sample are also quite different. Scanning electron studies of different amplification indicate that the size of the colloidal particles which form the aerogel remains practically the same up to 700°C while in the commercial product the particles shows a definite tendency to grow into larger particles[41].

### 4. Nb<sub>2</sub>O<sub>5</sub> AS PHOTOELECTRICAL COATING

Recently a new photovoltaic solar cell concept has been developed by Gratzel et al [42]. The device is based on the use of small (~ 20 nm) colloidal semiconductor particles of TiO<sub>2</sub> prepared by a sol-gel process and sintered at low temperature and whose superficial has been sensitized by a monolayer of transition metal complex in order to shift the absorption spectrum of TiO<sub>2</sub> (λ < 380 nm) toward the visible solar range. Contrary to conventional semiconductor cells, the nanocrystalline device separates the function of light absorption (charge creation) and charge transport. The light is first absorbed by the sensitizer whose absorption spectral range can be adapted to the solar spectral range by a careful choice of its composition. The excited electrons are then transferred to the conduction band of the TiO<sub>2</sub> where they rapidly diffuse through the thin coating (~ 2µm) and are collected by a conducting electrode. The cycle is then closed by returning the electrons to a counter electrode and through an adequate electrolyte which allows the regeneration of the sensitizer cations by electronic transfer. In such device, the TiO<sub>2</sub> coating has therefore two functions and act as a support for the sensitizing molecules and for the electronic charge transport.

Several other oxides present semiconducting properties including BaTiO<sub>3</sub>, WO<sub>3</sub>, Nb<sub>2</sub>O<sub>5</sub>, SrTiO<sub>3</sub>, KTaO<sub>3</sub>, Ta<sub>2</sub>O<sub>5</sub>, etc. Nb<sub>2</sub>O<sub>5</sub> can be obtained in form of small colloidal particles. The material has a band gap slightly larger than TiO<sub>2</sub> and the flat band potential vs SHE is 0V [43], slightly smaller than TiO<sub>2</sub> (0.2V).

The fabrication of 250 nm thick Nb<sub>2</sub>O<sub>5</sub> coating and the electrochemical test have been realized as described in section 2. However UV light from a 100 W Xe lamp was coupled to a Bausch and Lomb UV-

Visible high intensity monochromator and focussed on the sample through a quartz window adapted on the side of the electrochemical cell. Preliminary measurements show that niobate coatings present a photoelectric effect however less intense than TiO<sub>2</sub> coatings and may be of interest to substitute these coatings for the realization of solar cell similar to thos developed by Gratzel et al [44]

## 5. CONCLUSION

We have shown that it is possible to prepare Nb<sub>2</sub>O<sub>5</sub> materials by a sol-gel process either in the form of coating with excellent optical quality, xerogel or aerogel. The coatings heat treated at 560 °C in O<sub>2</sub> atmosphere present interesting electrochromic properties and turn blue under Li<sup>+</sup> ions insertion. The process is reversible for scan rate higher than 10 mV/s. Therefore these new coatings are very promising to substitute WO<sub>3</sub> coatings for the realization of smart windows and mirrors. Preliminary measurements also indicate that aerogels can be prepared with a higher surface area than the commercial CBMM product, a result very promising for catalytic purposes. Small colloidal particles have also been obtained and it was shown that this material presents a photoelectric effect when illuminating in the UV region. They are consequently promising to be used for photoelectrochemical applications such as the realization of nanocrystalline solar cells.

These researches were financially supported by grants of FAPESP, CNPq and FINEP (Brazil)

## 6. REFERENCES

1. Sakka, S.; Yoko, T., *Chemistry, Spectroscopy and Applications of Sol-Gel Glasses*, Reistfeld, R., Jorgensen, C. K., ed., Springer-Verlag, Berlin, p. 89-118, 1992
2. Agrawal, M.; Cronin, J. P.; Zhang, R., *SPIE Sol Gel Optics II*, San Diego, v. 1758, p. 330, 1992
3. Lyman, N.R.; Moser, F. H.; Hichwa, B.P., *SPIE Optical Materials Technology for Energy Efficiency Solar Energy Conversion IV*, v. 823, p. 130-7, 1987.
4. Lee, K.D., *J. Korean Phys. Soc.*, v. 24, p. 306-13
5. Bell, J. M.; Green, D. C.; Patterson, A.; Smith, G. B.; MacDonald, K. A.; Lee, K.; Kirkup, L. D.; Cullen, J. D.; West, B. O., *SPIE Optical Materials Technology for Energy Efficiency and Solar Energy Conversion X*, v. 1536, p. 2936, 1991.
6. Livage, J., *Solid State Ionics*, v. 50, p. 307-13, 1992.
7. Cronin, J. P.; Tarico, D. J.; Tonazzi, J. C. C.; Agrawal, A.; Kennedy, S. R., *SPIE Sol-Gel Optics II*, v. 1758, p. 343-59, 1992.
8. Green, D. C.; Bell, J. M.; Smith, G. B., *SPIE Sol-Gel Optics XI*, v. 1758, p. 26-30, 1992.
9. Sanchez, C., *Bol. Soc. Esp. Ceram. Vidrio*, v. 31, p. 191-9, 1992.
10. Cronin, J. P.; Tarico, D. J.; Tonazzi, J. C. C.; Agrawal, A.; Kennedy, S. R., *Solar Energy Materials and Solar Cells*, v. 29, p. 371-86, 1993.
11. Bell, J. M.; Smith, G. B.; Green, D. C.; Barczynska, J.; Evans, L.; MacDonald, D. A.; Voelkel, G.; West, B. O.; Spiccia, L., *SPIE Optical Materials Technology for Energy Efficiency and Solar Energy Conversion XI*, v. 2017, p. 132-42, 1993.
12. Chemseddine, A.; Morneau, R.; Livage, J., *Solid State Ionics*, v. 9-10, p. 357-62, 1983.
13. Xu, G.; Lhen, L., *Solid State Ionics*, v. 28-30, p. 1726-8, 1988.
14. Judenstein, P.; Livage, J., *Materials Science and Engineering*, v. 133, p. 129-32, 1989.
15. Yamamaka, K., *Japanese J. Applied Physics*, v. 20, p. 1307-8, 1981.
16. Oi, J.; Kishimoto, A.; Kudo, T., *J. Solid State Chemistry*, v. 96, p. 13-9, 1992.
17. Judenstein, P.; Livage, J., *SPIE Sol-Gel Optics*, v. 1328, p.344-51, 1990.
18. Hahli, M. A.; Glueck, D., *Solar Energy Materials*, v. 18, p. 127-41, 1989.
19. Uruma, H.; Tomooka, K.; Suzuki, Y.; Funasaki, T.; Kodera, K.; Matsushita, T., *J. Mat. Lett.*, v. 5, p. 1248-50, 1986.
20. Gottsche, J.; Hirsch, A.; Witterer, P., *SPIE Sol Gel Optics*, v. 1758, p. 13-25, 1991.
21. Macedo, M. A.; Dall'Antonia, L. H.; Aegerter, M. A., *SPIE Sol-Gel Optics II*, v. 1758, p. 320-9, 1992.
22. Macedo, M. A.; Aegerter, M. A., *J. Sol-Gel science and Technology*, to appear, 1994.
23. Goldner, R. B.; Seward, G.; Wong, K.; Haas, T.; Foley, G. H.; Chapman, R.; Schultz, S., *Solar Energy Materials*, v. 19, p. 17, 1988.
24. Ogan, S. F.; Randi, R. D., *SPIE*, v. 154, p. 482.
25. Judenstein, P.; Livage, J.; Zaudiansky, A.; Rose, R., *Solid State Ionics*, v. 28-30, p. 1722, 1988.
26. Nabavi, M.; Doeff, S.; Sanchez, C.; Livage, J., *Mater. Sci. Eng.*, v. B3, p. 203-7, 1989.
27. Nabavi, M.; Sanchez, C.; Livage, J., *Eur. J. Solid State Inorg. Chem.*, v. 28, p. 1173-92, 1991.
28. Katsuni, N.; Youchi, S.; Norio, M.; Noboru, Y., *J. Ceram. Soc. Jap.*, v. 101, p. 1032-7, 1993.
29. Doeff, S.; Sanchez, C., *Acad. Sci., Ser. 2*, v. 305, p. 531-4, 1989.
30. Ozer, N.; Chen, D. G.; Simmons, J. H., *Ceram. Trans (Glasses Electron. Appl.)*, v. 20, p. 253-63, 1991.
31. Slanger, V. L.; Orel, B.; Grabec, I.; Ogorec, B., *SPIE Optical Materials Technology for Energy Efficiency and Solar Energy Conversion XI Chromogenic for Smart Windows*, v. 1728, p. 118-29, 1992.
32. Reichman, B.; Bard, A. J., *J. Electrochem. Soc.*, v. 127, p. 241-2, 1979.
33. Gomes, M. A. B.; Bulhões, L. O. S.; Carstro, S. C.; Damião, A. J., *J. Electrochem. Soc.*, v. 137 (10), 3067-70, 1990.
34. Alves, M. do C., *MSc Thesis*, Federal University of São Carlos (Brazil), 1989.
35. Lee, R. G.; Gyaston, J. A., *J. Mater. Chem.*, v. 1, p. 381-6, 1991.
36. Bradley, D. C.; Chakravarti, B. N.; Wardlaw, W., *J. Am. Chem. Soc.*, v. 7, p. 2381-4, 1956.
37. Avelaneda, C. O.; Macedo, M. A.; Aegerter, M. A., *Proceedings of 38th. Congresso Brasileiro de Cerâmica*, Blumenau, SC, Brazil, 18-21/06/94.
38. Ko, E. I.; Weismann, J. G., *Catalysis Today*, v. 8, p. 27-36, 1990.
39. Weismann, J. G.; Ko, E. I.; Wymbhatt, P.; Howe, J. M., *J. Chem. Mat.*, v. 1, p. 187, 1989.
40. Fricke, J., ed., *Aerogel*, Springer-Verlag, 1986.
41. Rabelo, A. A.; Bozano, D. F.; Florentino, A.; Aegerter, M. A., *Proceedings of 38th. Congresso Brasileiro de Cerâmica*, Blumenau, SC, Brazil, 18-21/06/94.
42. Gratzel, M., *MRS Bulletin XVII*, v. 10, p. 61, 1993.
43. Kung, H. H.; Jarrel, H. S.; Sleight, A. W.; Ferretti, A., *J. Appl. Phys.*, v. 48, p. 2463, 1977.
44. Barros Filho, D. A.; Florentino, A.; Aegerter, M. A., *Proceedings of 38th. Congresso Brasileiro de Cerâmica*, Blumenau, SC, Brazil, 18-21/06/94.